

Phonon anomalies in trilayer high- T_c cuprate superconductors

Adam Dubroka^{*} and Dominik Munzar

*Institute of Condensed Matter Physics, Faculty of Science, Masaryk University,
Kotlářská 2, CZ-61137 Brno, Czech republic*

Abstract

We present an extension of the model proposed recently to account for dramatic changes below T_c (anomalies) of some c -axis polarized infrared-active phonons in bilayer cuprate superconductors, that applies to trilayer high- T_c compounds. We discuss several types of phonon anomalies that can occur in these systems and demonstrate that our model is capable of explaining the spectral changes occurring upon entering the superconducting state in the trilayer compound $\text{Ti}_2\text{Ba}_2\text{Ca}_2\text{Cu}_3\text{O}_{10}$. The low-temperature spectra of this compound obtained by Zetterer and coworkers display an additional broad absorption band, similar to the one observed in underdoped $\text{YBa}_2\text{Cu}_3\text{O}_{7-\delta}$ and $\text{Bi}_2\text{Sr}_2\text{CaCu}_2\text{O}_8$. In addition, three phonon modes are strongly anomalous. We attribute the absorption band to the transverse Josephson plasma resonance, similar to that of the bilayer compounds. The phonon anomalies are shown to result from a modification of the local fields induced by the formation of the resonance. The spectral changes in $\text{Ti}_2\text{Ba}_2\text{Ca}_2\text{Cu}_3\text{O}_{10}$ are compared with those occurring in $\text{Bi}_2\text{Sr}_2\text{Ca}_2\text{Cu}_3\text{O}_{10}$, reported recently by Boris and coworkers.

Key words: electron-phonon interaction, $\text{Ti}_2\text{Ba}_2\text{Ca}_2\text{Cu}_3\text{O}_{10}$, $\text{Bi}_2\text{Sr}_2\text{Ca}_2\text{Cu}_3\text{O}_{10}$, $\text{Ti}_2\text{Ba}_2\text{Ca}_2\text{Cu}_2\text{O}_8$

PACS: 74.25.Gz, 74.25.Kc, 74.72.Fq

1 Introduction

Some of the phonon modes in the high- T_c cuprate superconductors are strongly renormalized when going from the normal to the superconducting state [1,2,3,4,5,6,7,8,9,10].

^{*} fax: +420 541 211 214, tel: +420 541 129 378

Email addresses: dubroka@physics.muni.cz (Adam Dubroka),
munzar@physics.muni.cz (Dominik Munzar).

It is important to establish what particular type of electron-phonon interaction is responsible for these effects (so called phonon anomalies), and whether the anomalous phonons are “active players” in the mechanism of the high- T_c superconductivity [11,12,13] or whether they simply respond to changes of the electronic ground state that have an independent cause. Here we focus on the anomalies of c -axis polarized infrared-active phonons. The most pronounced of them have been observed in the so called multilayer compounds having two or more copper-oxygen planes per unit cell. Recently Munzar *et al.* [14] explained phonon anomalies in underdoped $\text{YBa}_2\text{Cu}_3\text{O}_{7-\delta}$ (Y-123). The explanation is based on the multilayer model of van der Marel and Tsvetkov [15,16,17], and the assumption of a weak (Josephson) coupling between the copper-oxygen planes: it has been assumed that the interlayer conductivities are fairly incoherent in the normal state and dominated by the coherent superfluid contribution in the superconducting state. A bilayer superconductor is thus considered as a superlattice of inter-bilayer and intra-bilayer Josephson junctions — this picture is called the Josephson superlattice model. The presence of two different junctions in a unit cell gives rise to a new transverse mode, the so called transverse Josephson plasma resonance (t-JPR) with a frequency between the one of the inter-bilayer (longitudinal) and the intra-bilayer (longitudinal) plasmon. The same picture of the c -axis charge dynamics of a bilayer system has also been arrived at by N. Shah and A.J. Millis [18] starting from a microscopic theory involving in-plane Green functions. An important new ingredient of the model of Ref. [14] is that the local field effects are taken into account: the changes of the phonon resonances in the infrared spectra result from changes of the (dynamical) local electric fields associated with the formation of the t-JPR. The same model, with a slightly different parameterization of the electronic contribution, has been more recently used to explain phonon anomalies in another bilayer compound, $\text{Bi}_2\text{Sr}_2\text{CaCu}_2\text{O}_z$ (Bi-2212) [5]. Very recently the t-JPR and the related phonon anomalies have also been observed in the trilayer compound $\text{Bi}_2\text{Sr}_2\text{Ca}_2\text{Cu}_3\text{O}_{10}$ [6] and briefly discussed in terms of the Josephson superlattice model and the local field effects. Here we present a detailed account of several types of phonon anomalies that can occur in trilayer cuprate superconductors (Sec. 2) and we compare our predictions with experimental data for the trilayer compound $\text{Tl}_2\text{Ba}_2\text{Ca}_2\text{Cu}_3\text{O}_{10}$ (Tl-2223) obtained by Zetterer *et al.* [7] (Sec. 3). Surprisingly, these data are found to be fairly different from those of $\text{Bi}_2\text{Sr}_2\text{Ca}_2\text{Cu}_3\text{O}_{10}$. In Sec. 4 we summarize our conclusions.

2 Theory

2.1 The basic concept and the response of a stack of superconducting CuO_2 planes

A schematic representation of the three CuO_2 planes of a trilayer compound and the basic structural element of Tl-2223 are shown in Fig. 1; E_{bl} and E_{int} denote the average electric fields in the intra-trilayer and the inter-trilayer region, respectively, and κ ($-\kappa$) denotes the surface charge density of the lower (upper) outer CuO_2 plane. The distance between the copper-oxygen planes in the trilayer block is denoted by d_{bl} and the distance between neighbouring trilayers by d_{int} . The magnitude of the inter-trilayer current density j_{int} is, due to the low conductivity of this region, much smaller than that of the intra-trilayer current density, j_{bl} . Consequently, j_{int} will be neglected ($j_{\text{int}} = 0$). Furthermore, the current density j_{bl} can be expressed as $j_{\text{bl}}(\omega) = -i\omega\epsilon_0\chi_{\text{bl}}(\omega)E_{\text{bl}}(\omega)$, where $\chi_{\text{bl}}(\omega)$ is the local susceptibility of the Josephson junction between the closely spaced CuO_2 layers. Because of symmetry, the local susceptibility is the same for both regions inside the trilayer block. As a consequence, the middle copper-oxygen plane does not become charged in an infrared wave; the fields and the current densities in the two regions are the same. The trilayer block behaves as one Josephson junction with the susceptibility $\chi_{\text{bl}}(\omega)$ connecting the outer planes of the block.

The c -axis dielectric function in the optical limit can be written as (cf. [19] p. 127)

$$\epsilon(\omega) = 1 + \frac{i}{\epsilon_0\omega} \frac{j(\omega)}{E(\omega)}, \quad (1)$$

where $j(\omega)$ and $E(\omega)$ are Fourier components of the total induced current density along the c -axis and the total electric field, respectively. Both variables are macroscopic, i.e., unit cell averages of the corresponding microscopic quantities. This equation can be written as

$$\epsilon(\omega) = \epsilon_\infty + \frac{i}{\epsilon_0\omega} \frac{\sum_k \langle j_k(\omega) \rangle}{E(\omega)}, \quad (2)$$

where ϵ_∞ is the interband dielectric constant, the induced current density is expressed as the sum of microscopic current densities $j_k(\omega)$ and the volume average is explicitly denoted by $\langle \rangle$. For a trilayer compound, Eq. (2) can be

further rewritten as

$$\epsilon(\omega) = \epsilon_\infty + \frac{2d_{\text{bl}}}{2d_{\text{bl}} + d_{\text{int}}} \frac{i}{\epsilon_0 \omega} \frac{j_{\text{bl}}(\omega)}{E(\omega)} + \frac{i}{\epsilon_0 \omega} \frac{\sum_k j_k^{\text{ph}}(\omega)}{E(\omega)}, \quad (3)$$

where the term $2d_{\text{bl}}/(2d_{\text{bl}} + d_{\text{int}})$ is the volume fraction of the intra-trilayer region and $j_k^{\text{ph}}(\omega) = -i\omega n_k Q_k r_k(\omega)$ represents the (volume averaged) current density due to vibrations of the ions of type k . Further n_k , Q_k and $r_k(\omega)$ are the corresponding concentration, effective dynamical charge, and displacement, respectively.

First we discuss the electronic part of the model, i.e., we set $j_k^{\text{ph}} = 0$. The electric fields E_{bl} and E_{int} shown in Fig. 1 a) are determined by the following equations

$$E_{\text{bl}}(\omega) = E'(\omega) + \frac{\kappa(\omega)}{\epsilon_0 \epsilon_\infty}, \quad (4)$$

$$E_{\text{int}}(\omega) = E'(\omega), \quad (5)$$

$$E(\omega) = \frac{2d_{\text{bl}}}{2d_{\text{bl}} + d_{\text{int}}} E_{\text{bl}}(\omega) + \frac{d_{\text{int}}}{2d_{\text{bl}} + d_{\text{int}}} E_{\text{int}}(\omega), \quad (6)$$

where E' is the component of the average internal field E that is due to external charges and depolarization processes at high frequencies. In the absence of the latter (i.e. for $\epsilon_\infty = 1$) E' would correspond to the field E_0 of Kittel's text book [20]. The continuity equation reads

$$j_{\text{bl}}(\omega) = i\omega \kappa(\omega). \quad (7)$$

Equations (4)–(7) are solved by

$$\frac{E_{\text{int}}(\omega)}{E(\omega)} = \frac{(2d_{\text{bl}} + d_{\text{int}}) \epsilon_{\text{bl}}(\omega)}{2d_{\text{bl}} \epsilon_\infty + d_{\text{int}} \epsilon_{\text{bl}}(\omega)}, \quad \frac{E_{\text{bl}}(\omega)}{E(\omega)} = \frac{(2d_{\text{bl}} + d_{\text{int}}) \epsilon_\infty}{2d_{\text{bl}} \epsilon_\infty + d_{\text{int}} \epsilon_{\text{bl}}(\omega)}, \quad (8)$$

$$\epsilon(\omega) = \frac{(2d_{\text{bl}} + d_{\text{int}}) \epsilon_\infty \epsilon_{\text{bl}}(\omega)}{2d_{\text{bl}} \epsilon_\infty + d_{\text{int}} \epsilon_{\text{bl}}(\omega)}, \quad (9)$$

where $\epsilon_{\text{bl}}(\omega) = \epsilon_\infty + \chi_{\text{bl}}(\omega)$.

In the following, the susceptibility χ_{bl} is taken in the form $\chi_{\text{bl}}(\omega) = -\omega_{\text{bl}}^2/\omega^2 + iS_{\text{bl}}/\omega$. The first and the second term represent the response of the superfluid and the background, respectively¹. The background is described in the

¹ It has been recently suggested [21] that the first term should be given a finite

simplest possible way (an infinitely broad Drude term) in order to keep the number of parameters small. Figure 2 shows the spectra of the real part $\sigma_1(\omega)$ of the optical conductivity $\sigma(\omega) = -i\omega\epsilon_0\epsilon(\omega)$ for several values of the plasma frequency ω_{bl} . Since this article aims at explaining the experimental data for Tl-2223, the following values characteristic for this compound have been used: $d_{\text{bl}} = 3.2 \text{ \AA}$, $d_{\text{int}} = 11.5 \text{ \AA}$, $A = a^2$, where $a = 3.9 \text{ \AA}$ is the in-plane lattice parameter [22]; further $\epsilon_\infty = 5$ (the value typical for the c -axis response of the high- T_c cuprates), and $S_{\text{bl}} = 1400 \text{ cm}^{-1}$ (a value, that gives a reasonable width to the t-JPR). The maximum in the spectra of Fig. 2 corresponds to the t-JPR. It can be seen that ω_{bl} determines not only the frequency of the resonance but also its spectral weight.

In order to include phonons, we have to take into account the local fields acting on the ions participating in the vibrations. It can be seen from Fig. 1 a) that the charge densities κ and $-\kappa$ give rise to three different electric fields: (a) the field between the trilayer blocks ($E_{\text{int}}^{\text{loc}}$), (b) the one inside the trilayer ($E_{\text{bl}}^{\text{loc}}$), and (c) the field at the outer copper-oxygen planes ($E_{\text{ocp}}^{\text{loc}}$). They are given as

$$E_{\text{int}}^{\text{loc}}(\omega) = E'(\omega) , \quad (10)$$

$$E_{\text{bl}}^{\text{loc}}(\omega) = E'(\omega) + \frac{\kappa(\omega)}{\epsilon_0\epsilon_\infty} , \quad (11)$$

$$E_{\text{ocp}}^{\text{loc}}(\omega) = E'(\omega) + \frac{\kappa(\omega)}{2\epsilon_0\epsilon_\infty} . \quad (12)$$

As a consequence, we arrive at three different elementary types of phonons consisting in vibrations of ions located in the three regions.

2.2 Vibrations of ions located in the inter- or intra-trilayer region

In order to include a phonon mode consisting in a vibration of a given type of ion, we have to express its contribution to the current density, j^{ph} , and describe its influence on the fields E_{bl} and E_{int} . For concreteness we focus on the inter-trilayer case; the intra-trilayer one can be treated in an analogical

spectral width, since it could be unrelated to the SC condensate. The suggestion was motivated by the observation that in strongly underdoped Y-123 the additional resonance, which is determined by this term, appears already at temperatures much higher than T_c . In other compounds, however, it starts to appear below T_c or very close to T_c . We are convinced that at least in the superconducting state the first term corresponds to the condensate. The origin of the above- T_c phenomena in strongly underdoped Y-123 is not yet clear but we believe that they are due to fluctuation effects.

way. The classical equation of motion for a particle of mass m and charge Q yields the following formula for the Fourier component of the displacement

$$r(\omega) = \frac{\epsilon_0 \chi(\omega) E_{\text{int}}^{\text{loc}}(\omega)}{nQ}, \quad (13)$$

where χ is the polarizability of the phonon,

$$\chi(\omega) = \frac{S_Q \omega_Q^2}{\omega_Q^2 - \omega^2 - i\omega\gamma_Q} \quad \text{with} \quad S_Q = \frac{nQ^2}{\epsilon_0 m \omega_Q^2}. \quad (14)$$

Further n is the density of the vibrating ions, $n = N/[A(2d_{\text{bl}} + d_{\text{int}})]$, where N is the number of the ions per volume $A(2d_{\text{bl}} + d_{\text{int}})$; ω_Q and γ_Q are the characteristic frequency and the broadening parameter, respectively. The (volume averaged) current density corresponding to this vibration is

$$j^{\text{ph}}(\omega) = -i\omega\epsilon_0\chi(\omega) E_{\text{int}}^{\text{loc}}(\omega). \quad (15)$$

The influence of the phonon on the electric fields can be taken into account using the following simple model: the planes of the ions are approximated by uniformly charged planes perpendicular to the c -axis with the same surface charge density, $\eta = NQ/A$ (see Fig. 3). Since the electric field generated by a uniformly charged plane does not depend on the distance from the plane, this assumption simplifies the model considerably. Using Fig. 3, we obtain the following equation for the average field in the inter-trilayer region:

$$d_{\text{int}} E_{\text{int}}(t) = [d_\eta + r(t)](-E_\eta) + [d_{\text{int}} - d_\eta - r(t)]E_\eta + d_{\text{int}} E'(t), \quad (16)$$

where d_η is the equilibrium distance of the charged plane from the lower CuO_2 plane, and $E_\eta = \eta/2\epsilon_0\epsilon_\infty$. Screening by high frequency processes is taken into account by ϵ_∞ in the denominator. Fourier transformation of Eq. (16) yields

$$\begin{aligned} E_{\text{int}}(\omega) &= E'(\omega) - \frac{r(\omega)}{d_{\text{int}}} \frac{\eta}{\epsilon_0\epsilon_\infty} = \\ &= E'(\omega) - \frac{\gamma}{\epsilon_\infty} \chi(\omega) E_{\text{int}}^{\text{loc}}(\omega), \quad \gamma = \frac{2d_{\text{bl}} + d_{\text{int}}}{d_{\text{int}}}. \end{aligned} \quad (17)$$

For the particular type of phonon Eq. (17) substitutes for Eq. (5), whereas Eq. (4) remains unchanged. The second term on the right-hand side of Eq. (17) represents the depolarization field of the phonon. Note that it contributes only to the field E_{int} and not to the field E_{bl} . On the other hand, the volume

averaged depolarization field

$$\frac{d_{\text{int}}}{2d_{\text{bl}} + d_{\text{int}}} \frac{\gamma}{\epsilon_{\infty}} \chi(\omega) E_{\text{int}}^{\text{loc}}(\omega) \quad (18)$$

is equal to $-P/\epsilon_0\epsilon_{\infty}$, where P is the macroscopic polarization [$P = \epsilon_0\chi(\omega)E_{\text{int}}^{\text{loc}}$]. This is the textbook formula for the macroscopic depolarization field (E_1 of Kittel's book) of a thin plate. The local fields $E_{\text{int}}^{\text{loc}}$, $E_{\text{bl}}^{\text{loc}}$, $E_{\text{ocp}}^{\text{loc}}$ do not contain any contribution of the depolarization fields. This resembles the exact cancellation of the depolarization field and the Lorentz field (E_2 of Kittel's textbook) that occurs in cubic crystals. Note that the phonon polarizabilities χ entering the model equations represent response functions with respect to the local fields instead of the averaged field. In the absence of interlayer currents, the input frequencies would correspond to the LO-frequencies while the frequencies renormalized according to the model equations would correspond to the TO-ones; considering only one phonon we obtain $\omega_{\text{TO}} = \omega_Q \sqrt{1 - S_Q/\epsilon_{\infty}}$. Note that if we include the current j^{ph} in Eq. (3), we also have to take into account the influence of the corresponding polarization on the electric field, i.e., the depolarization field. Otherwise the approach would not be consistent and may lead to unphysical results.

Figures 4 a) and 4 b) show the real part of the optical conductivity for two values of the phonon frequency, $\omega_Q = 320 \text{ cm}^{-1}$ and $\omega_Q = 610 \text{ cm}^{-1}$, respectively. The values of the remaining parameters correspond to O2 or O3 oxygens in Tl-2223: $N = 2$, $m = 16 \text{ amu}$, and we take $Q = -2|e|$ and $\gamma_Q = 20 \text{ cm}^{-1}$. The full lines represent the spectra of the normal state (NS) with $\omega_{\text{bl}} = 0$ and display only the phonon resonance. The dashed lines represent the spectra of the superconducting state (SCS) with $\omega_{\text{bl}} = 1400 \text{ cm}^{-1}$ and display both the t-JPR (the additional peak) and the phonon. We emphasize that the set of the values of the parameters used to compute the SCS spectrum differs from that of the NS only in the value of the parameter ω_{bl} . It can be seen that if the frequency of the phonon is lower than that of the t-JPR [Fig 4 a)], the spectral weight (SW) of the phonon is enhanced in the SCS. If it is higher [Fig 4 b)], the SW is reduced. Note that the qualitative characteristics of the anomaly depend only on the order of the two frequencies.

Next we consider a phonon consisting in a vibration of intra-trilayer ions of a given type. The derivation of the formula for the depolarization field is entirely analogical to the case of the inter-trilayer ions. We obtain

$$\begin{aligned} E_{\text{bl}}(\omega) &= E'(\omega) + \frac{\kappa(\omega)}{\epsilon_0\epsilon_{\infty}} - \frac{r(\omega)}{2d_{\text{bl}}} \frac{\eta}{\epsilon_0\epsilon_{\infty}} = \\ &= E'(\omega) + \frac{\kappa(\omega)}{\epsilon_0\epsilon_{\infty}} - \frac{\delta}{\epsilon_{\infty}} \chi(\omega) E_{\text{bl}}^{\text{loc}}(\omega), \quad \delta = \frac{2d_{\text{bl}} + d_{\text{int}}}{2d_{\text{bl}}}. \end{aligned} \quad (19)$$

This equation replaces Eq. (4) whereas Eq. (5) remains unchanged. The main difference from the inter-trilayer case is that the ions feel the local field $E_{\text{bl}}^{\text{loc}}$ instead of $E_{\text{int}}^{\text{loc}}$. Figures 4 c) and 4 d) show, how the phonon resonance is influenced by the superconducting transition. The values of the phonon frequencies are: $\omega_Q = 320 \text{ cm}^{-1}$ and 610 cm^{-1} , respectively. The values of the other parameters correspond to Ca in Tl-2223: $N = 2$, $m = 40 \text{ amu}$, and we take $Q = 2|e|$ and $\gamma_Q = 3 \text{ cm}^{-1}$. It can be seen that if the phonon frequency is lower than that of the t-JPR [Fig 4 c)], its SW is reduced and the phonon softens considerably. If it is higher [Fig 4 d)], the SW is enhanced and the phonon frequency increases. Note that the phonons are renormalized already in the NS because of the background term in the formula for χ_{bl} . The renormalization manifests itself, among others, in a non-Lorentzian shape of the resonances.

We have shown in Sec. 2.1 that the trilayer block behaves simply as a bilayer one with the interplanar distance of $2d_{\text{bl}}$. The approach presented here can thus be applied to both trilayer and bilayer compounds: in the latter case, $2d_{\text{bl}}$ in the coefficients γ and δ has to be substituted by d_{bl} and we have $\gamma = (d_{\text{bl}} + d_{\text{int}})/d_{\text{int}}$ and $\delta = (d_{\text{bl}} + d_{\text{int}})/d_{\text{bl}}$.

2.3 Vibrations of ions located in the outer CuO_2 planes of the trilayer block

For concreteness we further discuss the infrared-active (in-phase) vibrations of the oxygens O1 of the outer CuO_2 planes. Vibrations of the copper ions, however, can be treated in the same way. Boundaries between the intra- and inter-trilayer regions can be identified either with the static planes of the Cu ions or with the planes of the vibrating oxygens. In order to simplify our considerations we choose here the first approach. We have checked that for reasonable values of effective charges the use of the second one leads to very similar results. When expressing the depolarization fields in any of these approaches we encounter a problem: the interface between the inter- and the intra-trilayer regions is repeatedly crossed by a charged plane, which makes the time dependence of the fields E_{bl} and E_{int} unharmonic. This difficulty results from our approximation of the ionic planes by two-dimensional homogeneously charged planes. In order to get rid of the problem and keep the useful approximation at the same time, we represent the planar oxygens O1 by two homogeneously charged planes as shown in Fig. 5.

The surface charge density of each vibrating plane is $\eta/2$ with $\eta = N_{\text{O1}}Q_{\text{O1}}/A$, $N_{\text{O1}} = 2$. Following the derivation of the preceding section, we obtain the subsequent formula for the average field between the upper two CuO_2 planes of the trilayer:

$$\begin{aligned}
E_{\text{bl}}(\omega) &= E'(\omega) + \frac{\kappa(\omega)}{\epsilon_0 \epsilon_\infty} - \frac{r(\omega)}{d_{\text{bl}}} \frac{\eta/2}{\epsilon_0 \epsilon_\infty} = \\
&= E'(\omega) + \frac{\kappa(\omega)}{\epsilon_0 \epsilon_\infty} - \frac{2\alpha}{\epsilon_\infty} \chi_{\text{O1}}(\omega) E_{\text{ocp}}^{\text{loc}}(\omega), \quad \alpha = \frac{2d_{\text{bl}} + d_{\text{int}}}{4d_{\text{bl}}}. \quad (20)
\end{aligned}$$

We have used the relation between the displacement r and the local field $E_{\text{ocp}}^{\text{loc}}$, $r = \epsilon_0 \chi_{\text{O1}} E_{\text{ocp}}^{\text{loc}} / (n_{\text{O1}} Q_{\text{O1}})$ [cf. Eq. (13)], where n_{O1} is the concentration of the oxygens O1 of an upper CuO_2 plane, $n_{\text{O1}} = N_{\text{O1}} / [A(2d_{\text{bl}} + d_{\text{int}})]$. The average field between the two lower CuO_2 planes is also given by Eq. (20). Consequently, the central CuO_2 plane remains without time dependent charge density even for this type of vibration. The equation for the field E_{int} ,

$$\begin{aligned}
E_{\text{int}}(\omega) &= E'(\omega) - \frac{r(\omega)}{d_{\text{int}}} \frac{\eta}{\epsilon_0 \epsilon_\infty} = \\
&= E'(\omega) - \frac{2\beta}{\epsilon_\infty} \chi_{\text{O1}}(\omega) E_{\text{ocp}}^{\text{loc}}(\omega), \quad \beta = \frac{2d_{\text{bl}} + d_{\text{int}}}{2d_{\text{int}}} \quad (21)
\end{aligned}$$

can be obtained in an analogical way. Equations (20) and (21) substitute for (4) and (5). The current density due to the vibrating oxygens is given as the sum of the contributions of the two outer oxygen planes [cf. Eq. (15)]

$$j^{\text{ph}}(\omega) = -2i\omega\epsilon_0\chi_{\text{O1}}(\omega)E_{\text{ocp}}^{\text{loc}}(\omega). \quad (22)$$

The formulas for α and β of a bilayer system can be obtained along the lines of the considerations at the end of the previous subsection: $\alpha = (d_{\text{bl}} + d_{\text{int}})/2d_{\text{bl}}$ and $\beta = (d_{\text{bl}} + d_{\text{int}})/2d_{\text{int}}$.

Note that the second approach (with the boundaries associated with the charged planes of the planar oxygens) yields slightly different expressions for α and β in Eqs. (20) and (21) and also the formula for the current density due to the phonon differs from Eq. (22), see Appendix. In the previous works concerning bilayer systems Y-123 [14] and Bi-2212 [5,23], α and β have been calculated using the second approach but j^{ph} using the first one, i.e., Eq. (22). Fortunately, the errors caused by this formal inconsistency are negligible because the values of α and β resulting from both approaches are very close. Note that there are some errors in the third line of Table 1 of Ref. [14], the correct values will be published in an erratum [24].

Figure 6 a) and 6 b) shows the interplay between the t-JPR and the phonon for two values of the phonon frequency: $\omega_{\text{O1}} = 400 \text{ cm}^{-1}$ and 660 cm^{-1} . The values of the remaining parameters are $N_{\text{O1}} = 2$, $m_{\text{O1}} = 16 \text{ amu}$, and we take $Q_{\text{O1}} = -2|e|$ and $\gamma_{\text{O1}} = 20 \text{ cm}^{-1}$. If the phonon frequency is lower than that of the t-JPR [Fig 6 a)], the formation of the t-JPR is associated with a reduction of the phonon SW and its softening by about 5 cm^{-1} . An even more pronounced phonon anomaly of this type occurs for the bond bending mode

in underdoped Y-123 [14]. The fact, that the anomaly expected to occur in Tl-2223 is smaller than in Y-123, is connected to the difference in the width of the multilayer block. If the phonon frequency is higher than that of the t-JPR [Fig 6 b)], the SW of the phonon is enhanced in the SCS.

2.4 Composite vibrations

Up to this point we have described elementary vibrations where only one type of ion participates. This can be a good approximation for a mode where the major part of polarization is due to vibrations of one type of ion. For modes where several types of ions contribute significantly an extended version of the model is required. In this section we study composite modes of the oxygens of copper-oxygen planes. According to the results of the shell model calculations [26], in trilayer compounds such modes can be expected to occur.

In order to treat the composite modes as simply as possible we introduce the mechanical coupling scheme shown in Fig. 7, which provides an out-of-phase and an in-phase resonance. The equations of motion read

$$m_O \frac{d^2 r(t)}{dt^2} = -k_1 r(t) + k_2 [z(t) - r(t)] - m_O \gamma_{O1} \frac{dr(t)}{dt} + F_r(t) , \quad (23)$$

$$m_O \frac{d^2 z(t)}{dt^2} = 2k_2 [r(t) - z(t)] - m_O \gamma_{O4} \frac{dz(t)}{dt} + F_z(t) . \quad (24)$$

The forces F_r and F_z are proportional to the local fields: $F_r = E_{ocp}^{loc} Q_{O1}$ and $F_z = E_{bl}^{loc} Q_{O4}$. For the Fourier components of the ionic displacements we obtain

$$r(\omega) = \frac{F_r(\omega) q_z(\omega) + F_z(\omega) k_2}{q_r(\omega) q_z(\omega) - 2k_2^2} , \quad z(\omega) = \frac{F_z(\omega) q_r(\omega) + 2F_r(\omega) k_2}{q_r(\omega) q_z(\omega) - 2k_2^2} . \quad (25)$$

Here $q_r = -\omega^2 m_O + k_1 + k_2 - i\omega \gamma_{O1} m_O$, $q_z = -\omega^2 m_O + 2k_2 - i\omega \gamma_{O4} m_O$. The depolarization field for a composite vibration is the sum of the contributions of the elementary vibrations. Following the consideration of the previous subsections we obtain the equations for the mean fields:

$$E_{bl}(\omega) = E'(\omega) + \frac{\kappa(\omega)}{\epsilon_0 \epsilon_\infty} - \frac{r(\omega) \eta_{O1} + z(\omega) \eta_{O4}}{2d_{bl} \epsilon_0 \epsilon_\infty} , \quad (26)$$

$$E_{int}(\omega) = E' - \frac{r(\omega)}{d_{int}} \frac{\eta_{O1}}{\epsilon_0 \epsilon_\infty} , \quad (27)$$

where $\eta_{O1} = N_{O1} Q_{O1}/A$ and $\eta_{O4} = N_{O4} Q_{O4}/A$. Equations (26) and (27) again

replace Eqs. (4) and (5). The current density due to the vibrations of the oxygens is

$$\sum_k j_k^{\text{ph}}(\omega) = -2i\omega n_{\text{O1}} Q_{\text{O1}} r(\omega) - i\omega n_{\text{O4}} Q_{\text{O4}} z(\omega) . \quad (28)$$

The first and the second term on the right side of the Eq. (28) is due to vibrations of oxygens in the outer and inner copper-oxygen planes, respectively.

Figure 8 shows the real part of the optical conductivity for the model described above. The values of the parameters are: $N_{\text{O1}} = N_{\text{O4}} = 2$, $Q_{\text{O1}} = Q_{\text{O4}} = -2|e|$, $m_{\text{O}} = 16$, and we have chosen $\gamma_{\text{O1}} = \gamma_{\text{O4}} = 20 \text{ cm}^{-1}$, $k_2/k_1 = 0.3$ and $\omega_1 = \sqrt{\frac{k_1}{m}} = 320 \text{ cm}^{-1}$ (a), 600 cm^{-1} (b), 800 cm^{-1} (c), and 1100 cm^{-1} (d). The model yields an out-of phase (OPR) resonance and an in-phase (IPR) one. If the OPR frequency is lower than that of the t-JPR [Fig. 8 a)], its SW increases considerably when going from the normal to the SCS. On the contrary, if its frequency is higher [Fig. 8 b)], the SW of the phonon decreases. In both cases the phonon frequency remains approximately constant under the superconducting transition. For the IPR the situation is different: if its frequency is lower than that of the t-JPR [Fig. 8 b) and c)], its SW is strongly reduced and its frequency decreases. If the IPR frequency is higher [Fig. 8 d)], the changes are reverse: the SW increases and the phonon hardens. In Fig. 8 a) the interplay of the depolarization fields and the electronic background leads to a strong overdamping of the IPR. In Figs. 8 c) and d), the OPR is located above the displayed frequency range. It can be seen that the IPR frequency is renormalized much more than that of the OPR. This can be understood: for the IPR the displacements of the oxygens r and z have the same sign, therefore the depolarization field (the third term on the right-hand side of Eq. (26), determining the frequency shift, is large. On the contrary, for the OPR the signs of the displacements are opposite and the depolarization field is therefore small. Note that the qualitative aspects of the phonon anomalies of the composite modes are insensitive to changes of the value of the ratio k_1/k_2 .

The changes of the spectral weights reported in this section can be elucidated in terms of the changes of the local fields. Figure 9 displays frequency dependencies of the ratios $E_{\text{bl}}^{\text{loc}}/E$, $E_{\text{int}}^{\text{loc}}/E$ and $E_{\text{ocp}}^{\text{loc}}/E$ in the SCS obtained using Eqs. (4)–(12). The phonons have not been taken into account and $S_{\text{bl}} = 0$. The singularity at $\omega_p \approx 500 \text{ cm}^{-1}$ corresponds to the t-JPR. Since the values of the ratios in the NS are equal to one, their values in the SCS express the relative changes of the local fields when going from the NS to the SCS. Let us consider, e.g., the local field $E_{\text{int}}^{\text{loc}}$ that acts on ions situated in the inter-trilayer region. If the frequency ω_Q of a phonon involving vibrations of these ions is lower than ω_p , the local field $E_{\text{int}}^{\text{loc}}(\omega_Q)$ increases and the SW of the phonon increases [cf. Fig 4 a)]. If the frequency is higher, $E_{\text{int}}^{\text{loc}}(\omega_Q)$ decreases

and so does the spectral weight [cf. Fig 4 b)]. The SW changes of phonons consisting in a vibration of intra-trilayer ions or ions in the outer CuO_2 planes can be elucidated in a similar way. In order to understand the SW changes for a composite vibration of the planar oxygens, we have to take into account changes of the absolute values of the fields, changes of their relative signs, and the displacement pattern. In the frequency region $\omega_Q < \omega_p$, the local field $E_{\text{bl}}^{\text{loc}}$ changes sign under the superconducting transition while the sign of $E_{\text{ocp}}^{\text{loc}}$ remains unchanged, i.e., in the SCS the local fields are antiparallel in contrast to the NS, where they are parallel. Considering the out-of-phase resonance, the eigenvector pattern is in disagreement with that of the local field in the NS while they are in accord in the SCS. Consequently, the amplitude of the vibration is enhanced under the superconducting transition as well as the SW of the phonon [cf. Fig. 8 a)]. For the IPR the situation is reversed, i.e., the two patterns are in agreement in the NS while they disagree in the SCS. As a consequence, the SW of the phonon resonance decreases [cf. Fig. 8 c)]. For $\omega_Q > \omega_p$, the two local fields are parallel in both NS and SCS, and upon entering the SCS, their amplitudes increase. Since the eigenvector pattern of the in-phase resonance agrees with that of the electric field, its SW increases [cf. Fig. 8 d)].

The shifts of the phonon frequencies are related to the depolarization fields. Since the local fields shown in Fig. 9 have been obtained within a model, that does not incorporate the phonons, i.e., does not contain the depolarization fields, this picture cannot explain the shifts.

3 Comparison with experimental data and discussion

Pronounced phonon anomalies have been observed in the far-infrared spectra of the trilayer compound Tl-2223 [7]. In this section we discuss the experimental data, present an assignment of the phonon modes, and compare the experimental results with our predictions. Finally we comment on the phonon anomalies in $\text{Bi}_2\text{Sr}_2\text{Ca}_2\text{Cu}_3\text{O}_{10}$ (Bi-2223).

3.1 $\text{Tl}_2\text{Ba}_2\text{Ca}_2\text{Cu}_3\text{O}_{10}$

The conductivity spectra of Tl-2223 shown in Fig. 10 contain a structure situated on a high conductivity background. The spectra were obtained [7] by Kramers-Kronig transformation of reflectivity data of a ceramic sample consisting of microcrystals with random orientations. It is known, that sharper structures in the data of polycrystalline samples of high- T_c compounds corresponds largely to the c -axis polarized phonons and that the metallic back-

ground originates predominantly from the a - b conductivity (see [1] and Ref. therein). The absence of a - b polarized phonons can be seen, e.g., by comparing the reflectivity spectra of a ceramic Y-123 ceramic sample [25] with those of a c -axis oriented monocrystal [2]. The phonon structure (see Fig. 10) exhibits several changes under the superconducting transition: the SW of the phonon at 580 cm^{-1} decreases, a wide additional absorption band appears in the frequency region around 500 cm^{-1} , the SW of the phonon at 370 cm^{-1} increases, the frequency of the phonon at 305 cm^{-1} decreases by about 20 cm^{-1} , the SWs of the four low frequency phonons increase.

The lattice dynamical study of Tl-2223 [26] predicts eight infrared-active c -axes polarized phonons with eigenvectors shown in Fig. 11. Only seven phonon resonances, however, can be found in the normal state spectra of Fig. 10 a). We suggest that the phonon, that is not seen in the data, is the one with the predicted TO frequency of 443 cm^{-1} because we do not find any phonon around 443 cm^{-1} in the normal state spectra and because this mode should have a rather low oscillator strength. Having identified the missing phonon, we base the assignment of the phonons on the order of the TO frequencies. The differences between the measured and the predicted TO frequencies are within 20% which can be considered as a good agreement. Note however that also the results of the shell model calculations should be taken with some precaution. For example, the calculations do not consider free charge carriers.

As discussed in Sec. 2, the temperature evolution of a phonon resonance depends on whether its frequency is higher or lower than that of the t-JPR. We shall therefore identify the t-JPR in the conductivity spectrum and subsequently explain the observed changes of the phonons. We suggest that the additional absorption band appearing in the SCS around 500 cm^{-1} corresponds to the t-JPR. The band is rather wide (more than 100 cm^{-1}), similarly as in underdoped Y-123, and, in addition, located in the frequency region of no phonon related feature in the normal state data.

The major part of the polarization of the phonon at 580 cm^{-1} (the 583 cm^{-1} mode in Fig. 11) is due to the oxygens in the Tl-O layers. Vibrations of inter-trilayer ions have been described in Sec. 2.2, the corresponding model spectrum with the appropriate value of the phonon frequency is shown in Fig. 4 b). The calculation reproduces the experimentally observed decrease of the SW. Note, however, that the absolute values of the calculated and the measured conductivities cannot be compared because of the polycrystalline structure of the sample. In addition, in the model spectra of the SCS the phonon line appears as a shoulder on the background of the t-JPR; furthermore a weak broad band emerges at even higher frequencies. Both features seem to be present also in the experimental data. The latter can be interpreted as a part of the t-JPR, which is separated from the main part by the phonon. This feature is even more pronounced in the reflectivity data of the bilayer system

$\text{Ti}_2\text{Ba}_2\text{CaCu}_2\text{O}_8$ [27,28]. In the low temperature spectrum of this compound the t-JPR is centered at about 550 cm^{-1} but a part of it appears also around 700 cm^{-1} , above the phonon at 600 cm^{-1} .

The major part of the polarization of the 370 cm^{-1} mode of Fig. 10 is due to an out-of-phase vibration of the oxygens of the outer and the inner copper-oxygen planes (see the 383 cm^{-1} mode in Fig. 11). In section 2.3 we have described vibrations of the oxygens in the outer CuO_2 planes, the vibrations of those of the inner plane can be studied along the lines of Sec. 2.2. The corresponding model spectra are shown in Fig. 6 a) and Fig. 4 c), respectively. Both calculations yield a decrease of the SW and a softening of the phonon, in contrast with the experimental observation. However, for composite (out-of-phase) vibrations our model yields a SW increase without any frequency change [see Fig. 8 a)], in agreement with the experimental data. This agreement supports the local field picture discussed in the end of Sec. 2.4. In particular, it demonstrates dramatic spatial variations of the local electric field, even its sign changes on the scale of the inter-plane distance.

The polarization pattern corresponding to the phonon at 305 cm^{-1} (292 cm^{-1} mode in Fig. 11) is more complicated. The major part of its polarization is due to vibrations of the Ca ions and the apical oxygens. In section 2.2, we have described vibrations of intra-trilayer and inter-trilayer ions, the corresponding model spectra are shown in Fig. 4 c) and Fig. 4 a), respectively. Both exhibit a softening of the phonon, the former one shows in addition a SW decrease, similar to the one occurring in the experimental data. This suggests that the contribution of the Ca ions to the mode is more pronounced. The model spectrum of Fig. 4 c) shows a softening of about 40 cm^{-1} , much larger than the experimental value of 20 cm^{-1} . It is possible that the presence of other phonons in a more complete model would yield a lower value of the frequency shift. The SW predicted by the model is smaller than the experimental one, both in the NS and SCS. A better agreement could be probably obtained by considering a more complex polarization diagram. We have also to keep in mind the possibility that the mode at 305 cm^{-1} corresponds to the in-phase mode of the planar oxygens (the 443 cm^{-1} mode in Fig. 11), i.e., that the order of the in-phase and the out-of-phase mode is different from what is suggested by the shell model calculations. This seems to be the case in Bi-2223 [6]. The corresponding model spectrum shown in Fig. 8 b) exhibits a remarkable softening of the phonon resonance and the SW decrease as well.

Since the ceramic sample consist of randomly oriented microcrystals of the highly anisotropic material, the interpretation of the data is not straightforward. It is important to find out whether the above discussed spectral changes are intrinsic features of the crystal or artefacts induced by the polycrystalline structure. The reflectivity of polycrystalline $\text{Ti}_2\text{Ba}_2\text{CuO}_6$ with one CuO_2 layer per formula unit (see Fig. 12 in Ref. [27]) exhibits only very small differences

between above and below T_c , but the structures over 250 cm^{-1} in the data of the double layer compound ($\text{Tl}_2\text{Ba}_2\text{CaCu}_2\text{O}_8$) and the triple layer compound (Tl-2223) change considerably (see Fig. 13 and 15 of Ref. [27]). We are therefore convinced that the main changes of the phonon structures are intrinsic effects rather than artifacts. However, some spectral characteristics must be influenced by the polycrystalline structure. We suggest that it is the reason of the unexpectedly large values of the SW of phonons [7] and the anomalies of the three low frequency modes.

3.2 A remark on the phonon anomalies in $\text{Bi}_2\text{Sr}_2\text{Ca}_2\text{Cu}_3\text{O}_{10}$

Recently A. V. Boris *et al.* [6] reported the far-infrared c -axis spectra of the trilayer compound Bi-2223, that has the same crystal structure as Tl-2223. It is interesting to find out whether the phonon anomalies of this compound can also be explained by using the model introduced above, especially those of the two modes that are specific to the trilayer compounds: the in-phase and the out-of phase oxygen bond bending modes. A qualitative explanation of the SW changes has already been presented in Ref. [6]. It is further interesting to explore the differences between the spectra of the two compounds.

In the SCS spectra of Bi-2223, a broad additional absorption band appears around 500 cm^{-1} (see Fig. 1 of Ref. [6]) which has been attributed to the t-JPR. Results of the shell model calculations suggest that the spectral structures at 360 cm^{-1} and at 400 cm^{-1} correspond to the in-phase and the out-of-phase oxygen bond-bending modes, respectively. The SW of the former decreases in the SCS, in contrast to the SW of the latter, that increases below T_c . The two features are in qualitative agreement with our predictions [see Figs. 8c) and 8a), respectively]. The observed softening of the phonon at 360 cm^{-1} (about 5 cm^{-1} , the value of the shift is doping dependent), however, is considerably smaller than in our model calculations. It may be due to a coupling between the phonon and the pronounced mode at 305 cm^{-1} , mediated by the depolarization fields, that is not included in our model.

The main differences between the spectra of Tl-2223 and Bi-2223 are: (a) The spectra of Tl-2223 exhibit only three phonon related structures at frequencies above 250 cm^{-1} . This is in contrast with Bi-2223, where four main phonon bands have been found. (b) The mode at 305 cm^{-1} in Bi-2223 has a large SW and its contribution to the spectra is almost temperature independent. No such mode exists in Tl-2223. (c) The spectral weight of the t-JPR in Tl-2223 seems to be much larger than in Bi-2223 as described below.

Measurements on a single-crystal allowed the authors of Ref. [6] to obtain the SW of the t-JPR as the difference between the integrated SCS and NS

spectra. For a Bi-2223 sample with $T_c = 102$ K that has approximately the same frequency of the t-JPR as the Tl-2223 sample studied in [7], the SW of the t-JPR is approximately $1100 \Omega^{-1} \text{cm}^{-2}$. Concerning Tl-2223, we estimate that the SW is about $8000 \Omega^{-1} \text{cm}^{-2}$ from the area between the 115 K and the 25 K spectra as shown in Fig. 10 d). The SW in Tl-2223 is thus several times larger than in Bi-2223. It must be of course affected by the ceramic nature of the sample, nevertheless, it can be seen even by comparison with the strongest phonons in the spectrum that the SW is fairly large. The SW of the t-JPR predicted by our model is $18\,000 \Omega^{-1} \text{cm}^{-2}$. This prediction is about twice as much as the observed value for Tl-2223, but the value for Bi-2223 is an order of magnitude lower. We emphasize, that the SW of the t-JPR in our model is not an arbitrary parameter but is determined by the frequency of the t-JPR (see Fig. 2). The reason why the infrared spectra of Tl-2223 and of Bi-2223 differ so much is not yet understood and remains as an open question for future investigations.

4 Summary and conclusions

We have extended the model of Ref. [14] that accounts for phonon anomalies occurring in bilayer compounds to trilayer high- T_c superconductors and discussed several possible phonon anomalies that can occur in these systems. The model explains the experimental infrared data of the trilayer high- T_c compound Tl-2223 obtained by Zetterer *et al.* [7]. The broad maximum that appears in the conductivity spectra below T_c and represents the dominant feature of the low temperature spectra corresponds to the transverse Josephson plasma resonance. The phonon anomalies can be explained in terms of changes of the local electric fields induced by the formation of the resonance. Of particular interest is the anomaly of the 370cm^{-1} mode, i.e., the large increase of its spectral weight below T_c . We recall that this mode consists in an out-of-phase vibration of the planar oxygens and is thus specific to the trilayer compounds. Its anomalous behavior is due to the fact that the displacement pattern does not agree with the pattern of the local field in the normal state, but it does agree with the one of the superconducting state, where the sign of the field changes from the inner CuO_2 plane to the outer one.

The qualitative and in some cases even quantitative agreement between the predictions of our model and the experimental data indicates that the model captures well the underlying mechanism. According to the model, the anomalies are caused by a change of the electronic ground state associated with a crossover of the c -axis dynamics from incoherent to coherent, the change which would presumably occur even in the absence of any electron-phonon coupling. It seems thus that the anomalous infrared-active phonons are passive rather than active players in the mechanism of superconductivity.

The spectra of Tl-2223 are qualitatively similar to those of Bi-2223 reported by Boris *et al.*: both exhibit the additional absorption band and the anomalies of three high-frequency phonons. The magnitudes of the effects, as far as we can conclude based on the data of polycrystalline Tl-2223, are considerably different. This suggests that the spacing layers of the two materials possess fairly different electronic properties.

Acknowledgements

We acknowledge discussions with J. Humlíček and C. Bernhard. The work has been supported by the project MSM 143100002 of the Ministry of Education of Czech Republic.

A Appendix

Here we present the formulas of the approach where boundaries are associated with the charged planes of the planar oxygens. Equations (20) and (21) remain as they are with

$$\alpha = - \left(\frac{\eta_{\text{tl}} + \eta_{\text{Cu}}}{\eta_{\text{O}}} \right) \frac{2d_{\text{bl}} + d_{\text{int}}}{4d_{\text{bl}}} \quad (\text{A.1})$$

$$\beta = - \left(\frac{\eta_{\text{int}} + \eta_{\text{Cu}}}{\eta_{\text{O}}} \right) \frac{2d_{\text{bl}} + d_{\text{int}}}{4d_{\text{int}}} \quad (\text{A.2})$$

where η_{tl} (η_{int}) is the total surface charge density of the intra-trilayer (inter-trilayer) region, i.e., the sum of the densities of the charged planes located inside this region. Further η_{Cu} (η_{O}) is the surface charge density of the Cu ions (O ions) of a CuO_2 plane. Equation (22) is substituted by

$$j^{\text{ph}}(\omega) = -2i\omega\epsilon_0\chi_{\text{O1}}(\omega)E_{\text{ocp}}^{\text{loc}*}(\omega) \quad (\text{A.3})$$

with

$$E_{\text{ocp}}^{\text{loc}*}(\omega) = E' + \frac{\kappa(\omega)}{2\epsilon_0\epsilon_\infty} \frac{4d_{\text{bl}}}{2d_{\text{bl}} + d_{\text{int}}} \alpha. \quad (\text{A.4})$$

The formulas for α , β , and $E_{\text{ocp}}^{\text{loc}*}$ of a bilayer system can be obtained by substituting $2d_{\text{bl}}$ by d_{bl} .

References

- [1] A.P. Litvinchuk, C. Thomsen and M. Cardona, *Physical Properties of High Temperature Superconductors IV*, editor D.M. Ginsberg Singapore World Scientific 1994.
- [2] C.C. Homes, T. Timusk, D.A. Bonn, R. Liang and W.N. Hardy, *Physica C* **254** (1995) 265.
- [3] J. Schützmann, S. Tajima, S. Miyamoto, Y. Sato and R. Hauff, *Phys. Rev. B* **52** (1995) 13 665.
- [4] C. Bernhard, D. Munzar, A. Golnik, C.T. Lin, A. Wittlin, J. Humlíček, M. Cardona, *Phys. Rev. B* **61** (2000) 618.
- [5] V. Železný, S. Tajima, D. Munzar, T. Motohashi, J. Shimoyama, and K. Kishio, *Phys. Rev. B* **63** (2001) 060502.
- [6] A.V. Boris, D. Munzar, N.N. Kovaleva, B. Liang, C.T. Lin, A. Dubroka, A.V. Pimenov, T. Holden, B. Keimer, Y.-L. Mathis and C. Bernhard, *Phys. Rev. Lett.* **89** (2002) 277001.
- [7] T. Zetterer, M. Franz, J. Schützman, W. Ose, H.H. Otto, and K.F. Renk, *Phys. Rev. B* **41** (1990) 9 499.
- [8] V.G. Hadjiev, Xingjiang Zhou, T. Strohm, M. Cardona, Q.M. Lin and C.W. Chu, *Phys. Rev. B* **58** (1998) 1043.
- [9] M. Limonov, S. Lee, S. Tajima, A. Yamanaka, *Phys. Rev. B* **66** (2002) 054509.
- [10] J.H. Chung, T. Egami, R.J. McQueeney, M. Yethiraj, M. Arai, T. Yokoo, Y. Petrov, H.A. Mook, Y. Endoh, S. Tajima, C. Frost, F. Dogan, *Phys. Rev. B* **67** (2003) 014517.
- [11] M.L. Kulić, *Physics Reports* **338** (2000) 1-264.
- [12] A. Lanzara, P.V. Bogdanov, X.J. Zhou, S.A. Kellar, D.L. Feng, E.D. Lu, T. Yoshida, H. Eisaki, A. Fujimori, K. Kishio, J.I. Shimoyama, T. Noda, S. Uchida, Z. Hussain, Z.X. Shen, *Nature* **412** (2001) 510.
- [13] Z.X. Shen, A. Lanzara, S. Ishihara, N. Nagaosa, *Philosophical Magazine B* **82** (2002) 1349.
- [14] D. Munzar, C. Bernhard, A. Golnik, J. Humlíček, M. Cardona, *Solid State Commun.* **112** (1999) 365.
- [15] D. van der Marel and A. Tsvetkov, *Czechoslovak Journal of Physics* **46** (1996) 3165.
- [16] M. Grüninger, D. van der Marel, A.A. Tsvetkov, and A. Erb, *Phys. Rev. Lett.* **84** (2000) 1575.
- [17] D. van der Marel and A.A. Tsvetkov, *Phys. Rev. B* **64** 024530.

- [18] N. Shah and A.J. Millis, Phys. Rev. B **65** (2001) 024506.
- [19] H. Ehrenreich, in *The Optical Properties of Solids*, Proceedings of the International School of Physics “Enrico Fermi”, Course XXXIV, Varenna, 1965, edited by J. Tauc (Academic Press, New York, 1996), Chap. 13.
- [20] Charles Kittel, *Introduction to Solid State Physics* (John Wiley & Sons Inc., 1976, 5. edition), Chap. 13.
- [21] T. Timusk, C.C. Homes, Solid State Commun. **126** (2003) 63.
- [22] M. Hasegawa, Y. Matsushita, H. Takei, Physica C **267** (1996) 31.
- [23] D. Munzar, C. Bernhard, T. Holden, A. Golnik, J. Humlíček and M. Cardona, Phys. Rev. B **64** (2001) 024523.
- [24] D. Munzar *et al.*, unpublished.
- [25] L. Genzel, A. Wittlin, M. Bauer, M. Cardona, E. Schönherr, and A. Simon, Phys. Rev. B **40** (1989) 2170.
- [26] A.D. Kulkarni, F.W. de Wette, J. Prade, U. Schröder a W. Kress, Phys. Rev. B **41** (1990) 6 409.
- [27] K.F. Renk, in *Thallium-Based High-Temperature Superconductors*, editor A.M. Hermann, J.V. Yakhmi, (Marcel Dekker Inc. New York 1994).
- [28] K.F. Renk, W. Ose, T. Zetterer, J. Schutzmann, H. Lengfellner, H.H. Otto, J. Keller, B. Roas, L. Schultz, G. Saemannischenko, Infrared physics **29** (1989) 791.

Figure captions:

Fig. 1. a) Schematic representation of the model of a trilayer superconductor. The CuO_2 planes are approximated by homogeneously charged planes. The symbol κ ($-\kappa$) denotes the surface charge density of the upper (lower) CuO_2 plane. b) The basic structural element of $\text{Tl}_2\text{Ba}_2\text{Ca}_2\text{Cu}_3\text{O}_{10}$ [22]. The oxygens in the outer (inner) CuO_2 planes are labelled as O1 (O4), the oxygens in the BaO (TlO) planes as O2 (O3).

Fig. 2. Real part of the c -axis conductivity of the electronic part of the model for the following values of the intra-trilayer plasma frequency ω_{bl} : 0 (normal state), 400, 700, 1000 and 1400 cm^{-1} . It can be seen that ω_{bl} determines not only the frequency of the transverse Josephson plasma resonance, but also its spectral weight.

Fig. 3. Schematic representation of our approach to treat the influence of the phonon polarization on the electric field. The plane of ions of a given type is approximated by the uniformly charged plane with the same charge per unit area η . The displacement of the plane from its equilibrium position (dashed line) is denoted by r . The electric field due to the charged plane is labelled as $\pm E_\eta$, $E_\eta = \eta/(2\epsilon_0\epsilon_\infty)$.

Fig. 4. Anomalies of a phonon consisting in a vibration of ions situated in the inter-trilayer region [a) and b)] or in the intra-trilayer region [c) and d)]. The solid (dashed) lines correspond to the normal (superconducting) state. The transverse Josephson plasma resonance is labelled as t-JPR and the phonon resonance as $\text{P}_{\text{O}3}$ and P_{Ca} in Figs. a), b) and c), d), respectively. The values of the parameters used in the computations are given in the text.

Fig. 5. The scheme used for the evaluation of the depolarization fields of the oxygen-bond bending mode. The oxygens of an outer CuO_2 plane are represented by two homogeneously charged planes.

Fig. 6. Anomalies of a phonon consisting in vibrations of the oxygens of the outer CuO_2 planes. The dashed (solid) lines correspond to the normal (superconducting) state. The transverse Josephson plasma resonance is labelled as t-JPR and the phonon resonance as $\text{P}_{\text{O}1}$. The values of the parameters used in the computations are given in the text.

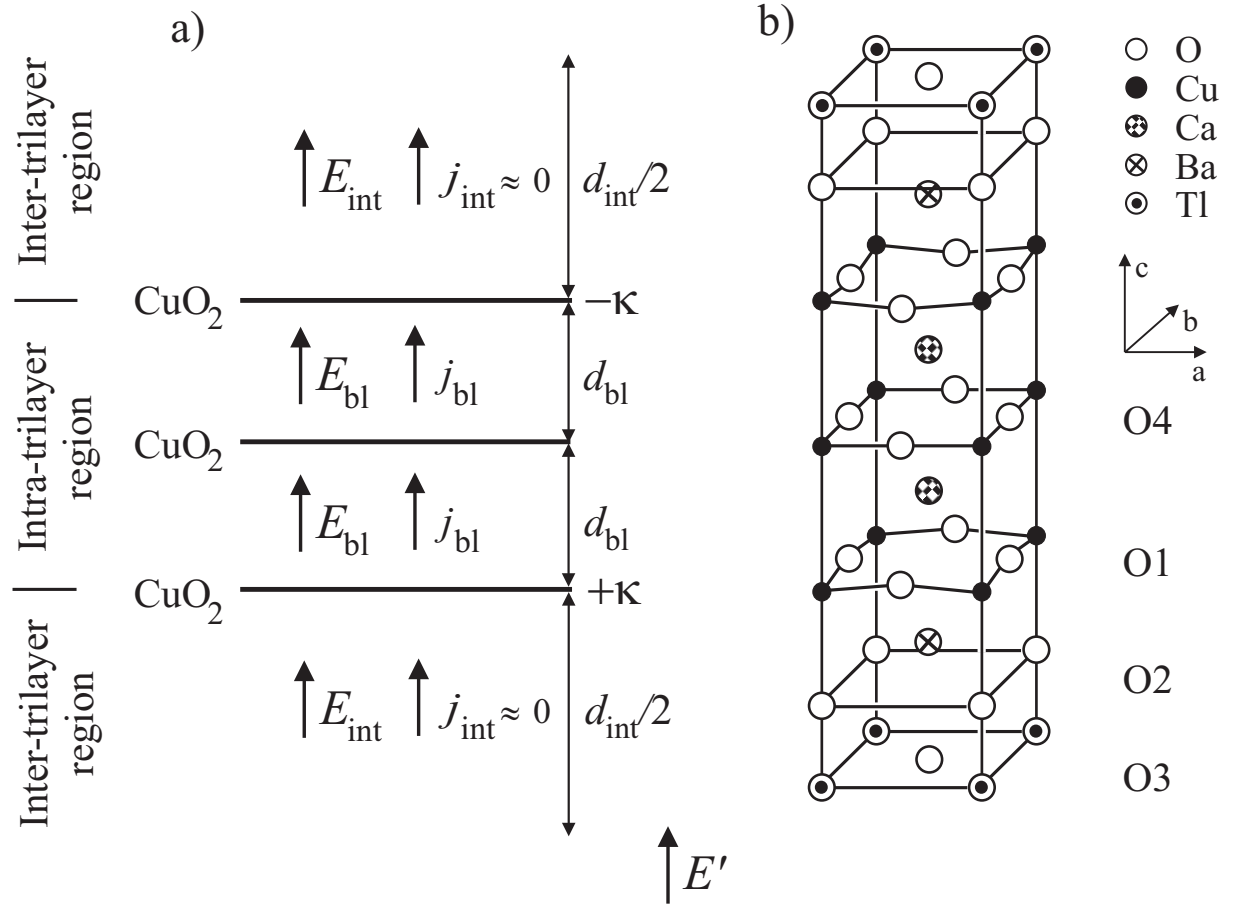
Fig. 7. String model used to describe the composite vibrations of the planar oxygens. The displacement of the oxygens O1 (O4) from their equilibrium position is labelled as $r(z)$, the string constants are denoted by k_1 and k_2 . The local electric fields $E_{\text{ocp}}^{\text{loc}}$ ($E_{\text{bl}}^{\text{loc}}$) act on the oxygens O1 (O4).

Fig. 8. Anomalies of the in-phase resonance (IPR) and the out-of-phase resonance (OPR) of the planar oxygens. The dashed (solid) lines correspond to the normal (superconducting) state. The transverse Josephson plasma resonance is labelled as t-JPR. The values of the parameters used in the computations are given in the text.

Fig. 9. Frequency dependencies of the normalized local electric fields in the superconducting state. The symbols $E_{\text{int}}^{\text{loc}}$, $E_{\text{bl}}^{\text{loc}}$ and $E_{\text{ocp}}^{\text{loc}}$ denote the local fields in the inter-trilayer region, inside the trilayer, and on the outer cuprate planes, respectively. The normalized local fields acting on the ions participating in the modes at 305, 380 and 580 cm^{-1} , are indicated by A, B, and C, respectively.

Fig. 10. Conductivity spectra of $\text{Tl}_2\text{Ba}_2\text{Ca}_2\text{Cu}_3\text{O}_{10}$ ($T_c = 112\text{ K}$) adapted from Ref. [7]. The spectra have been obtained by Kramers-Kronig transformation of reflectivity data of a ceramic sample. Part d) contains the spectra of part b) and c). The shaded area between the 115 K and the 25 K spectra gives us an rough estimate of the spectral weight of the transverse Josephson plasma resonance.

Fig. 11. Eigenvector diagrams of the c -axis polarized infrared-active phonons of $\text{Tl}_2\text{Ba}_2\text{Ca}_2\text{Cu}_3\text{O}_{10}$ with the corresponding TO (LO) frequencies obtained by shell model calculations in Ref. [26].



Dubroka *et al.* Fig. 2

